AD-A148 830 ACTA AERONAUTICA ET ASTRONAUTICA SINICA (SELECTED ARTICLES)(U) FOREIGN TECHNOLOGY DIV WRIGHT-PATTERSON AFB OH C LIU ET AL. 27 NOV 84 FTD-ID(RS)T-1150-84 1/1

UNCLASSIFIED F/G 20/4 NL

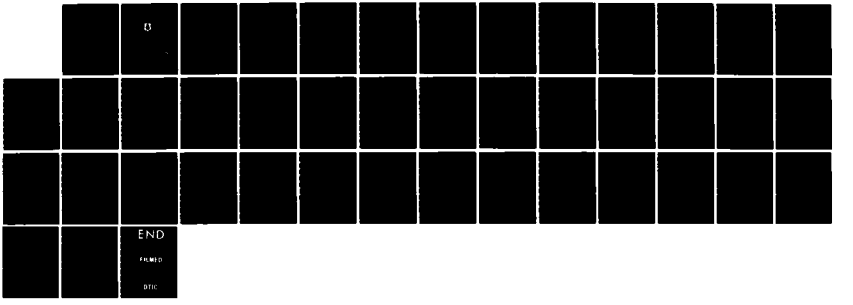

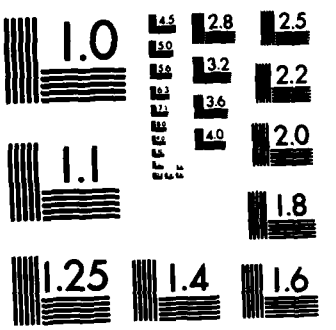

FTD-ID(RS)T-1150-84

FOREIGN TECHNOLOGY DIVISION

ACTA AERONAUTICA ET ASTRONAUTICA SINICA

(Selected Articles)

Approved for public release;
distribution unlimited.

EDITED TRANSLATION

FTD-ID(RS)T-1150-84 27 November 1984

MICROFICHE NR: FTD-84-C-001116

ACTA AERONAUTICA ET ASTRONAUTICA SINICA
(Selected Articles)

English pages: 38

Source: Hangkong Xuebao, Vol. 5, Nr. 1, 1984, pp. 11-29

Country of origin: China
Translated by: SCITRAN
F33657-81-D-0263
Requester: FTD/TQTA

PREPARED BY:

TRANSLATION DIVISION
FOREIGN TECHNOLOGY DIVISION
WP-AFB, OHIO.

Table of Contents

GRAPHICS DISCLAIMER

All figures, graphics, tables, equations, etc. merged into this translation were extracted from the best quality copy available.

An Approximated Solution of the Aircraft Lateral-Directional Limit Cycle Oscillation Induced by Aerodynamic Hysteresis**

*/11

Nanjing Aeronautical Institute Liu Chang

ABSTRACT

This paper gives the approximated analytical equation and determines the characteristics of the aircraft lateral-directional limit cycle oscillations which are induced by aerodynamic hysteresis. Our computation indicates that it agrees fairly well with the result obtained by the numerical iteration method in references [1,2]. Furthermore, our method eliminates the shortcoming in the references mentioned above in that the amplitude of cycle oscillation associated with the roll rate limit is not the maximum amplitude.

I. INTRODUCTION

References [1,2] pointed out that during wind tunnel experiments both the roll in the lateral direction and the yawing moment vary with the yaw angle under the conditions of separation of gas flow from the surface of the wing of the aircraft at high angles of attack. Under these conditions there also exists the phenomenon of hysteresis. This model is shown in Figure 1.

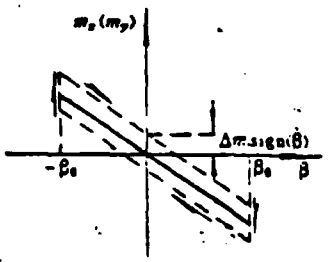

Figure 1. Aerodynamic Rolling (Yawing) Moment Hysteresis

*Numbers in margin indicate foreign pagination

**Received September 1983

12

The moment coefficient induced by yawing is

$$m_i = m_i^{\beta}\beta + \Delta m_i \operatorname{sign}(\dot{\beta}), \qquad i = x, y \tag{A}$$

In this equation $m_i^{\beta}\beta$ is the moment coefficient induced by yawing when the phenomenon of hysteresis does not exist, Δm_i is the increment of the rolling moment coefficient produced by hysteresis. This increment is close to a sudden instantaneous change, comparable to a relay effect. Its magnitude is a constant and its direction varies with the sideslip angle velocity $\dot{\beta}$. By using the state variable analysis method of the control theory and under the condition of neglecting the side force equation from the equation of motion in the direction lateral to the motion, references [1,2] obtained the period and amplitude of the lateral-directional limit cycle oscillation based on a numerical iteration method. By using the linealized harmonic wave method of the control theory, this paper linealized the nonlinear relay type moment increment produced by hysteresis. This paper then applied the equilibrium method of harmonic waves [3] to obtain the analytical representative equations of the frequency and amplitude of the limit cycle oscillation based on the simplified lateral equation of motion. From the approximated equation, the effects of the moment increment induced by hysteresis and the related aerodynamic derivatives are very obvious. This is very convenient to the analysis of the characteristics of the limit cycle oscillation. The result of the computation indicates that the result given by the approximated analytical equation is in good agreement with the result given by references [1,2].

The rules of the aerodynamic manual [4] will be followed for all the symbols which are used in this paper but not explained explicitly. Further discussion on the related references [1,2] can be found in reference [5].

II. COMPUTATIONAL METHOD

We will consider the side force equation for the lateral perturbating motion of the aircraft. We will also assume that the attack angle and all control surfaces remain unchanged.

In this way we can obtain $I_z\frac{d\omega_z}{dt}=M_z^{\beta}\beta+M_z^{\omega_y}\omega_y+M_z^{\omega_z}\omega_z$ /12

$$I_y\frac{d\omega_y}{dt}=M_y^{\beta}\beta+M_y^{\omega_y}\omega_y+M_y^{\omega_z}\omega_z \qquad (B)$$

If the aircraft maintains a straight flight path, $\omega_y = d\psi/dt=d\beta/dt=\dot{\beta}$, and the equation shown above can be simplified into

$$\left.\begin{aligned}\ddot{\beta}&=\bar{M}_y^{\beta}\beta+\bar{M}_y^{\dot{\beta}}\dot{\beta}+\bar{M}_y^{\omega_z}\omega_z\\ \dot{\omega}_z&=\bar{M}_z^{\beta}\beta+\bar{M}_z^{\dot{\beta}}\dot{\beta}+\bar{M}_z^{\omega_z}\omega_z\end{aligned}\right\} \qquad (1)$$

The derivatives in this equation have short lines on top of them, indicating that these derivatives are divided by their corresponding rolling moments, such as $\bar{M}_y^{\beta}= M_y^{\beta}/I_y$, $\bar{M}_x^{\beta}= M_x^{\beta}=M_x^{\beta}/I_x$

The nonlinear additional moment coefficient m is induced by aerodynamic hysteresis is the relay type, as shown in Figure 2. We can obtain the equivalent moment coefficient derivative by using the linearized harmonic wave method[3] . It can be represented as:

$$\Delta m_i^{\dot{\beta}}=\frac{4\Delta m_i}{\pi\omega_1\theta_1} \qquad (C)$$

Or we can also represent it as the moment derivative:

$$\Delta\bar{M}_i^{\dot{\beta}}=\frac{4\Delta\bar{M}_i}{\pi\omega_1\theta_1} \qquad (2)$$

In this equation $\Delta\bar{M}_i = \Delta M_i qsl/I_i$, i = x,y and θ_1, ω_1 are the amplitude and frequency of the limit cycle oscillation.

By substituting the increment of the hysteresis moment derivative (2) into equation (1), we can obtain the equation which considers the equation of lateral perturbating motion under the influence of mement hysteresis.

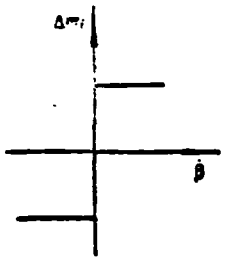

Figure 2. Nonlinear Additional Moment Coefficient.

1. Rolling Moment Hysteresis

After taking the additional increment of the rolling hysteresis moment $\bar{\Delta M}_x^{\dot{\beta}}$ into consideration, equation (1) can be written in the following form:

$$\left.\begin{aligned}\ddot{\beta} &= \bar{M}_\beta^{\beta}\beta + \bar{M}_{\dot\beta}^{\beta}\dot\beta + \bar{M}_{\omega_x}^{\beta}\omega_x \\ \dot\omega_x &= \bar{M}_\beta^{\omega_x}\beta + \left(\bar{M}_{\dot\beta}^{\omega_x} + \frac{4\Delta\bar{M}_x}{\pi\omega_1\theta_1}\right)\dot\beta + \bar{M}_{\omega_x}^{\omega_x}\omega_x\end{aligned}\right\} \quad (3)$$

By eliminating ω_x from equation (3), we can get

$$\dddot{\beta} = (\bar{M}_{\dot\beta}^{\dot\beta} + \bar{M}_{\omega_x}^{\omega_x})\ddot{\beta} + \left[\bar{M}_\beta^{\dot\beta} + \bar{M}_{\dot\beta}^{\omega_x}\left(\bar{M}_\beta^{\dot\beta} + \frac{4\Delta\bar{M}_x}{\pi\omega_1\theta_1}\right) - \bar{M}_{\omega_x}^{\omega_x}\bar{M}_{\dot\beta}^{\dot\beta}\right]\dot\beta + (\bar{M}_{\dot\beta}^{\omega_x}\bar{M}_\beta^{\dot\beta} - \bar{M}_{\omega_x}^{\omega_x}\bar{M}_\beta^{\dot\beta})\,\beta \quad (4)$$

Based on the harmonic wave equilibrium method [3], we can assume the approximated solution of the limit cycle oscillation to have the following form. We then have

$$\left.\begin{aligned}\beta &= \theta_1\cos\omega_1 t \\ \dot\beta &= -\theta_1\omega_1\sin\omega_1 t \\ \ddot\beta &= -\theta_1\omega_1^2\cos\omega_1 t \\ \dddot\beta &= \theta_1\omega_1^3\sin\omega_1 t\end{aligned}\right\} \quad (5)$$

Substituting equation (5) into equation (4) and after rearranging, we have /13

$$\theta_1\omega_1^2\sin\omega_1 t=\{-(\bar{M}_\beta^{\dot\beta}+\bar{M}_\alpha^{\dot\alpha})\theta_1\omega_1^2+(\bar{M}_\beta^{\dot\alpha}\bar{M}_\alpha^{\beta}-\bar{M}_\alpha^{\dot\alpha}\bar{M}_\beta^{\beta})\theta_1\}\cos\omega_1 t \qquad (D)$$
$$-\left\{\bar{M}_\beta^{\beta}+\bar{M}_\beta^{\dot\alpha}\left(\bar{M}_\alpha^{\dot\beta}+\frac{4\Delta\bar{M}_x}{\pi_1\omega\theta_1}\right)-\bar{M}_\alpha^{\dot\alpha}\bar{M}_\beta^{\dot\beta}\right\}\theta_1\omega_1\sin\omega_1 t$$

By comparing the corresponding first order harmonic wave coefficients on two sides of the equation above, we have

$$\theta_1\omega_1^2=-\left\{\bar{M}_\beta^{\beta}+\bar{M}_\beta^{\dot\alpha}\left(\bar{M}_\alpha^{\beta}+\frac{4\Delta\bar{M}_x}{\pi\omega_1\theta_1}\right)-\bar{M}_\alpha^{\dot\alpha}\bar{M}_\beta^{\beta}\right\}\theta_1\omega_1 \qquad (6)$$

$$0=-(\bar{M}_\beta^{\dot\beta}+\bar{M}_\alpha^{\dot\alpha})\theta_1\omega_1^2+(\bar{M}_\beta^{\dot\alpha}\bar{M}_\alpha^{\beta}-\bar{M}_\alpha^{\dot\alpha}\bar{M}_\beta^{\beta})\theta_1 . \qquad (7)$$

From equation (7) we can obtain the frequency of limit cycle oscillation at sideslip angle β as

$$\omega_1=\left(\frac{\bar{M}_\beta^{\dot\alpha}\bar{M}_\alpha^{\beta}-\bar{M}_\alpha^{\dot\alpha}\bar{M}_\beta^{\beta}}{\bar{M}_\beta^{\dot\alpha}-\bar{M}_\alpha^{\dot\alpha}}\right)^{1/2}. \qquad (8)$$

By substituting equation (8) into equation (6), we can obtain the corresponding amplitude of the limit cycle oscillation as

$$\theta_1=-\frac{4\Delta\bar{M}_x\bar{M}_\beta^{\dot\alpha}}{\pi\omega_1(\omega_1^2+\bar{M}_\beta^{\beta}+\bar{M}_\beta^{\dot\alpha}\bar{M}_\alpha^{\beta}-\bar{M}_\alpha^{\dot\alpha}\bar{M}_\beta^{\beta})} . \qquad (9)$$

From the above equation, it is clear that the magnitude of the amplitude of limit cycle oscillation is directly proportional to the additional rolling moment $\Delta\bar{M}_x$ induced by the aerodynamic hysteresis.

From the first equation in equation (3), we can obtain

$$\omega_x=\frac{1}{\bar{M}_\beta^{\dot\alpha}}(\ddot\beta-\bar{M}_\beta^{\beta}\beta-\bar{M}_\beta^{\dot\beta}\dot\beta). \qquad (10)$$

We now substitute equation (5) into equation (10), after rearranging the equation we can get

$$\omega_x=\frac{1}{\bar{M}_\beta^{\dot\alpha}}\{\bar{M}_\beta^{\dot\beta}\theta_1\omega_1\sin\omega_1 t-(\theta_1\omega_1^2+\bar{M}_\beta^{\beta}\theta_1)\cos\omega_1 t\}, \qquad (E)$$

Let $C = \bar{M}_y^{\beta}\theta_1\omega_1/\bar{M}_y^{\omega_x}$, $C_2 = -(\theta_1\omega_1 + \bar{M}_y^{\beta}\theta_1)/\bar{M}_y^{\omega_x}$, the above equation can be rewritten as:

$$C_1 = \bar{M}_y^{\dot{\beta}}\theta_1\omega_1/\bar{M}_y^{\omega_x}, \quad C_2 = -(\theta_1\omega_1^2 + \bar{M}_y^{\beta}\theta_1)/\bar{M}_y^{\omega_x}.$$
$$\omega_x = C_1\sin\omega_1 t + C_2\cos\omega_1 t = \theta_1\sin(\omega_1 t + \varphi_1) \tag{11}$$

In this equation we have

$$\theta_2 = \sqrt{C_1^2 + C_2^2}$$
$$\varphi_1 = \operatorname{tg}^{-1}\frac{C_2}{C_1} \tag{F}$$

According to equation (11) we can determine the amplitude of the limit cycle oscillation θ_2 at the rolling speed ω_x as

$$\theta_2 = \frac{\theta_1}{\bar{M}_y^{\omega_x}}\sqrt{(\bar{M}_y^{\dot{\beta}}\omega_1)^2 + (\omega_1^2 + \bar{M}_y^{\beta})^2}. \tag{12}$$

From the equation above we can see that the oscillating amplitude θ_2 at rolling speed ω_x is linearly proportional to the oscillation θ_1 at sideslip angle β.

2. Yawing moment hysteresis

After taking into consideration the additional increment of the yawing hysteresis moment derivative $\Delta\bar{M}_y^{\beta}$, equation (1) can be rewritten into the following form

$$\left.\begin{aligned}\ddot{\beta} &= M_y^{\dot{\beta}}\dot{\beta} + \left(\bar{M}_y^{\beta} \pm \frac{4\Delta\bar{M}_z}{\pi\omega_2\theta_2}\right)\beta - M_y^{\omega_x}\omega_x \\ \dot{\omega}_x &= \bar{M}_x^{\dot{\beta}}\dot{\beta} - M_x^{\beta}\beta - M_x^{\omega_x}\omega_x\end{aligned}\right\}. \tag{13}$$

/14

By eliminating ω_x from equation (13), we can get

$$\ddot{\beta} = \left(\bar{M}_y^{\dot{\beta}} + M_x^{\omega_x} + \frac{4\Delta\bar{M}_z}{\pi\omega_2\theta_2}\right)\ddot{\beta} + \left(M_y^{\beta} + \bar{M}_y^{\omega_x}M_x^{\dot{\beta}} - M_x^{\omega_x}\bar{M}_y^{\dot{\beta}} - M_x^{\omega_x}\frac{4\Delta\bar{M}_z}{\pi\omega_2\theta_2}\right)\dot{\beta}$$
$$+ (\bar{M}_y^{\omega_x}M_x^{\beta} - \bar{M}_x^{\omega_x}\bar{M}_y^{\beta})\beta \tag{14}$$

Based on the same principle and according to the harmonic wave equilibrium method, the frequency ω_2 of the limit cycle oscillation at sideslip angle β can be obtained from the equation above

$$\omega_2 = \left(\frac{-(A_1B_0 - A_0B_1) \pm \sqrt{(A_1B_0 - A_0B_1)^2 - 4A_1B_1C_1}}{2A_1}\right)^{1/2} \tag{15}$$

$$A_0 = \bar{M}_y^{\beta} - \bar{M}_z^{\omega_x}$$

$$A_1 = \frac{4}{\pi} \Delta \bar{M}_y$$

$$B_0 = \bar{M}_y^{\beta} + \bar{M}_y^{\omega_y} \bar{M}_z^{\omega_x} - \bar{M}_y^{\omega_x} \bar{M}_z^{\omega_y} \qquad (G)$$

$$B_1 = -\frac{4}{\pi} \Delta \bar{M}_y \bar{M}_z^{\omega_y}$$

$$C_0 = \bar{M}_y^{\omega_y} \bar{M}_z^{\beta} - \bar{M}_z^{\omega_y} \bar{M}_y^{\beta}$$

and the amplitude of the limit cycle oscillation θ_3

$$\theta_3 = -\frac{4 \Delta \bar{M}_y \omega_x}{\pi (A_0 \omega_x^2 - C_0)} \qquad (16)$$

We can see from equation (16) that the magnitude of the amplitude θ_3 is directly proportional to the increment of the yawing hyteresis moment.

Similarly, after taking the additional increment of the yawing hysteresis moment derivative $\Delta \bar{M}_y^{\beta}$ into consideration, we can determine the amplitude θ_4 of the limit cycle oscillation at rolling rate ω_x.

$$\theta_4 = \frac{\theta_3}{\bar{M}_y^{\omega_y}} \sqrt{\left[\left(\bar{M}_y^{\omega_y} + \frac{4 \Delta \bar{M}_y}{\pi \omega_x \theta_3}\right) \omega_x\right]^2 + (\omega_x^2 - \bar{M}_y^{\beta})^2} \qquad (17)$$

From the equation above we can see that the amplitude of oscillation θ_4 at rolling rate ω_x is directly proportional to the amplitude of oscillation θ_3 at sideslip angle β .

3. The Amplitude and Frequency at Rolling Angle

According to the approximated relationship equation $d\gamma/dt = \omega_x$, we can determine the amplitude of the limit cycle oscillation θ_γ at rolling angle γ as

$$\theta_\gamma = \theta_{\omega_x} / \omega \qquad (18)$$

In this equation $\theta\omega_x$ and ω are the amplitude and frequency of the rolling rate limit cycle oscillation.

III. SAMPLE CALCULATION AND ANALYSIS

By taking the data set corresponding to the landing state of the F-94A aircraft as reference [1,2] did, we can compute the corresponding moment derivatives as:

$\bar{M}_x^{\beta} = -2.8256$ 1/second $\quad \bar{M}_y^{\beta} = -1.3214$ 1/second

$\bar{M}_{\omega x}^{\omega} = -2.4593$ 1/second $\quad M_y^{\omega} = 0.06283$ 1/second

$\bar{M}_x^{\omega y} = -1.5193$ 1/second $\quad \bar{M}_y^{\omega y} = \bar{M}_y^{\dot{\beta}} = -0.2489$ 1/second

According to the equations derived earlier, we can compute the amplitude θ and period T ($= \frac{2\pi}{\omega}$) of the rolling and yawing lateral-directional cycle oscillation induced by hysteresis. The results are shown in Table 1. For easy comparison, we have also listed the results obtained by the numerical iteration method of reference [2] in Table 1. /15

2. 迟滞类型		13. 幅值	14. 幅值
3. 迟滞大小		$\Delta\bar{M}_x = 1$	$\Delta\bar{M}_y = 0.05$
4. θ_β(弧度)	7. 按本文解析公式	0.0931	0.2115
	8. 按文献[2]数值迭代	0.0922	0.2105
5. θ_{m_β}(1/弧度)	9. 按本文解析公式	0.4230	0.2586
	10. 按文献[2]数值迭代	0.2948	0.2551
6. T(秒)	11. 按本文解析公式	5.5854	5.3142
	12. 按文献[2]数值迭代	5.5977	5.3459

1. Table 1. Amplitudes and Periods of Sideslip Angles and Roll Rate Limit Cycle Oscillations

2. type of hysteresis
3. magnitude of hysteresis
4. θ_β(radian)
5. θ^β (1/radian)
6. T(second)
7. according to our paper's analytical equation
8. according to the numerical iteration method of reference [2]
9. according to our paper's analytical equation
10. according to the numerical iteration of reference [2]
11. according to our paper's analytical equation

12. according to the numerical iteration method of reference [2]
13. rolling
14. yawing

From this table we can see that:

(1) The period of the limit cycle oscillation T computed based on the analytical equation proposed by this paper is very close to the period obtained by using the numerical iteration method of reference [2].

(2) With the exception of the $\theta_{\cdot_z}$ induced by rolling hysteresis $\Delta\bar{M}_x$, the amplitude of the limit cycle oscillation computed based on the analytical equation proposed by this paper is also in good agreement with the computed one based on the numerical iteration method of reference [2]. Reference [2] gave the computer simulated result of the lateral equation of perturbating motion (1) which takes into consideration the moment increment induced by hysteresis. The curves of the transitional processes are shown in Figures 3 and 4. The results show the reliability of the approximation method.

(3) The amplitude $\theta_{\cdot_z}$ of the rolling rate limit cycle induced by the rolling hysteresis as computed by the method of this paper ($\approx$0.42) is higher than the value computed by the numerical iteration method of reference [2] (0.29). But we can see from Figure 3 that it is relatively close to the $\theta_{\cdot_z}$ value obtained by an integration of the original numerical value of the equation ($\approx$0.38). Actually, the $\theta_{\cdot_z}$ value obtained from the numerical iteration method of reference [2] is a value corresponding to the condition where $\dot{\beta}$ vanishes to zero. This corresponds to the lower peak value in Figure 3, not the maximum amplitude of the rolling rate limit cycle oscillation. Of course, the computational result of the analytical equation will inevitably bring in a certain amount of error since the rolling rate reaction differs from the wave form of the first order harmonic wave significantly under certain conditions.

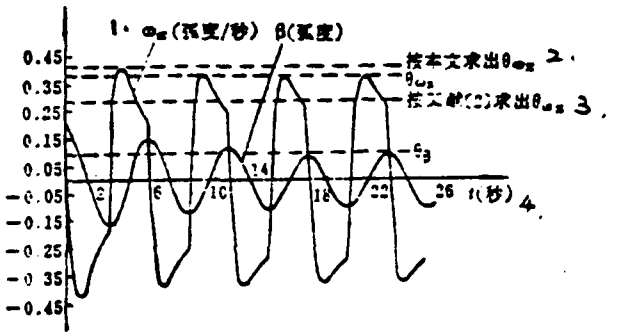

Figure 3. Limit Cycle Oscillation Induced by Rolling Hysteresis

1. ω_x (radian/second) β (radian)
2. $\theta\omega_x$ computed according to this paper
3. $\theta\omega_x$ computed according to reference [2]
4. t(second)

Similarly, we have also conducted computations by using the $\theta\omega_x$ and T values in Table 1 in the approximation equation (18) which determines the rolling angle r and amplitude θ_r. The results obtained are also relatively satisfactory.

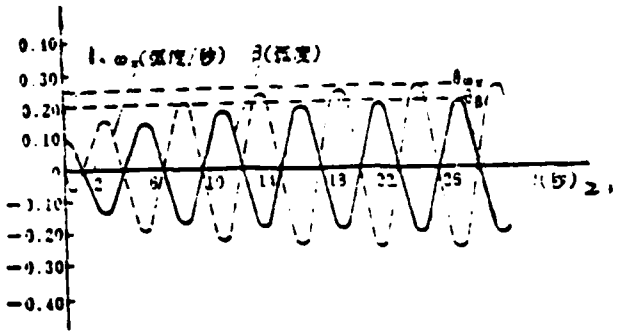

Figure 4. Limit Cycle Oscillation Induced by Yawing Hysteresis

1. ω_x(radian/second) β (radian)
2. t^*(second)

IV. CONCLUSION

The approximated analytical equation in this paper can be used to determine the characteristics of the lateral-directional limit cycle oscillation induced by aerodynamic hysteresis. The results of the computation indicate that they are in good agreement with the results obtained by using the numerical iteration method of references [1,2]. This paper also avoids the shortcoming of these references in that the amplitude of the roll rate limit oscillation induced by rolling hysteresis is not the maximum amplitude. In addition to the simplicity in computation, the analytical equation is convenient for the analysis of the effects of the magnitude of hysteresis and the various related aerodynamic derivatives on the characteristics of the limit cycle oscillation since the equation is very explicit.

Professor Tan Zhen Hua has provided many valuable comments. We wish to express our appreciation here.

REFERENCES

[1] L.V. Schmidt, Wing Rock Due to Aerodynamic Hysteresis, Journal of Aircraft, Vol. 16, No. 3 (1979).

[2] P.D. Young, Wing Rock as a Lateral-Directional Aircraft Limit Cycle Oscillation Induced by Nonlinear Aerodynamics Occuring at High Angle of Attack, AD A042104, (1977).

[3] D.W. Jordan & P.S. Mith, Nonlinear Ordinary Differential Equations, Oxford University Press, (1977).

[4] Compiling Section of the Aerodynamic Navigation Manual, Volume 1, (1975).

[5] Liu Chang, Limit Cycle Oscillation of Aircraft, (Journal of the Nanjing Aeronautical Institute), Volume 2 (1982).

Liu Chang

(Nanjing Aeronautical Institute)

Abstract

Wind tunnel tests on aircraft models often demonstrate that the variation of lateral-directional rolling and yawing moments with the yaw angle gives evidence of aerodynamic hysteresis occurred at high angle of attack. The non-linear additional increments of the moment due to aerodynamic hysteresis are linearized by the harmonic linear method. Then, based on the harmonic balance method, an approximate analytical formula is derived for determining the characteristics of aircraft lateral-directional limit cycle oscillation induced by aerodynamic hysteresis. Calculations by this method show that the results are in good agreement with data obtained by the numerical iterating method in references[1]and[2]. The method eliminates the shortcoming in the above references that the amplitude of roll rate limit cycle oscillation induced by roll hysteresis is not the maximum.

Selection of the Longitudinal Feedback Coefficients of the Stability Augmentation System in Order to Improve Riding Qualities**

/18

Northwestern Polytechnical University Gao Hao

ABSTRACT

The longitudinal feedback coefficients of a stability augmentation system (SAS) for a sample aircraft were selected based on the condition that the normal acceleration response at the pilot's position was approximately zero. The improvement in riding qualities was estimated based on references [2.3]. In addition, the dynamic characteristics of the combined aircraft-SAS system were also analyzed. The results indicate that the requirement of riding quality could be satisfied when the control anticipative parameter (CAP) of the combined aircraft-SAS system was close to $9.81/l_x$, and that the working range of the SAS was within 10% of the maximum inclination angle of the flat tail. If the area of the flat tail was relatively large compared to the area of the wing, such as when $\overline{Y}^{b_z}/\overline{Y}^{\alpha} \geqslant 0.2$, the lift term due to the elevator deflection would have to be considered in the analysis of the dynamic characteristics of the combined aircraft-SAS system.

INTRODUCTION

For aircrafts which will have to take low altitude combat missions, the design of the exterior arrangement of the aircraft alone is generally not going to be enough to satisfy the requirement of riding quality. The results of our analysis and computation indicate that we should try to improve the riding quality of the aircraft mainly by trying to reduce the normal acceleration response at the pilot's position when the aircraft is flying in atmospheric turbulence. In order to achieve this, we can introduce various types of automatic devices in the longitudinal passage of the aircraft. The effects of the various

** Received March, 1983

types of automatic devices on the improvement of riding quality can be found in reference [3]. By using a certain type of intercepting fighter as an example, this paper analyzed several problems involving the selection of the feedback coefficients of the stability augmentation system (SAS) using the improvement in riding quality of the aircraft by the longitudinal SAS as a guide. The standards of the aircraft riding qualities used in this paper followed the related specification of the United States Military manual MIL-F-8785B.

I. The Selection of the Feedback Coefficients of the Longitudinal Augmentation System Used to Improve Riding Quality

In principle, we can satisfy the standard of riding quality by using various ways to select the feedback coefficients of the stability augmentation system. Here we will only discuss the selection of the feedback coefficients of centered SAS based on the criterion that the requirement of riding quality be satisfied.

If we can use the short period equation of motion to approximately describe the dynamic characteristics of the aircraft, and we can take the diving angular velocity of the aircraft reaction, the attack angle, and the increment of the loading coefficient in the normal direction as the feedback signals, the regulatory principle of the SAS under ideal conditions is

$$\Delta\delta_e = K_\alpha \Delta\alpha + K_\omega \omega_z + K_n \Delta n_y \qquad \text{(A)}$$

The block diagram of the combined aircraft-SAS system is shown in Figure 1.

In order to simplify the discussion, we will not consider the dynamic characteristics of the auxiliary propeller and steering mechanism. This is to say that we will set $G_1 = G_2 = 1$. From this we can transform Figure 1 into

$$\frac{\Delta n_y}{\Delta P_x} = \frac{K_p \frac{V}{g} \bar{Y}^{\alpha} \bar{M}_z^{\delta_z}}{s^2 + 2\zeta\omega s + \omega^2} \qquad (B)$$

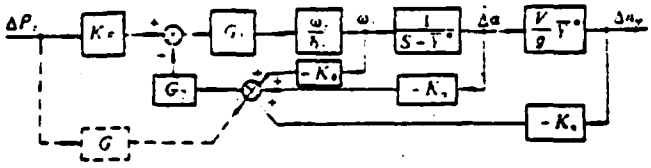

图 1　飞机-增稳器系统方框图

1. Figure 1. Block diagram of the aircraft-SAS System.
2. In this figure, G_1, G_2 are the transmission function of the auxiliary propeller and steering mechanism, respectively;
3. Enlargement coefficient and transmission function which are related to the force of the pilot control stick;
4. K_a, $K_{\dot{\vartheta}}$, K_n - the feedback coefficient of the attack angle, the inclination angle, and the loading coefficient;
5. $\omega_z / \delta_z = \Delta\dot{\vartheta} / \Delta du$ -transmission function of the aircraft.

$$\Delta\dot{\vartheta} = \bar{M}_z^{\delta_z}(S - \bar{Y}^{\alpha})$$
$$\Delta_{dz} = S^2 + 2\zeta_{dz}\omega_{dz}S + \omega_{dz}^2$$

In this equation we have

$$2\zeta\omega = 2\zeta_{dz}\omega_{dz} - K_{\dot{\vartheta}}\bar{M}_z^{\delta_z}$$
$$\omega^2 = \omega_{dz}^2 - \bar{M}_z^{\delta_z}\left[\bar{Y}^{\alpha}\left(K_{\dot{\vartheta}} + \frac{V}{g}K_n\right) + K_a\right] \qquad (C)$$

From this we can see that the introduction of the $\dot{\vartheta}$, $\Delta x y$, $\Delta\alpha$ signals is equivalent to a change in the frequency of the short period mode of the aircraft, while only the introduction of the $\dot{S}$ signal can change the damping of the short periodic state.

In principle, we can select any arbitrary combination of K_a, $K_{\dot{\vartheta}}$ and K_n to satisfy the requirement of the short period mode described above. Here we will start our analyses from the requirement of the riding quality of the aircraft. This is to say that we will start from the condition that the normal-directional loading coefficient reaction at the pilot's position be kept at a minimum.

We will assume that under the action of exterior perturbation the increment of the normal-directional loading coefficient reaction at the center of mass of the aircraft can be represented by Δn_y, the angular acceleration can be represented as $\dot{\omega}_z$, and the distance between the pilot's seat and the center of mass of the aircraft is l_x. The condition which guarantees the normal-directional loading reaction at the pilot's position to be zero is

$$\Delta n_y + \frac{l_x}{g}\dot{\omega}_z = 0 \qquad \text{(D)}$$

After simplification and some transformation which is not complicated, the condition above can be rewritten as

$$\frac{\omega^2}{\left(\frac{n_y}{\alpha}\right)_{s\to\infty}} = \text{CAP} \approx \frac{g}{l_x} \qquad \text{(E)}$$

Generally speaking, l_x are smaller than 9.81 meters for fighters, attack planes and figther bombers. This is why we can expect the CAP values obtained from the equation above to satisfy the standard of riding quality.

By expanding the ω^2 and (n_y/α), $s\to\infty$ terms, we can ultimately obtain the condition which determines CAP as

$$\frac{g}{l_x} \approx \text{CAP} = \frac{g}{V}\left\{\omega_{sp}^2 - \bar{M}_\alpha^{\cdot}\left[\bar{Y}_\alpha^{\cdot}\left(K_\theta + \frac{V}{g}K_\alpha\right) - K_\alpha\right]\right\} \qquad \text{(F)}$$

For simplicity, we can set K_θ and K_n to have a constant proportionality relationship. In other words /20

$$K = K_\alpha / K_\theta \qquad \text{(G)}$$

The value of K can be determined through a sample calculation. At the same time, we believe that the introduction of the K_α signal primarily compensates for the effect of the variation in the intrinsic frequencies of the short period modes of the

aircraft when the aircraft is flying under different M numbers. Because of this, we can select K_{ao} by using

$$\omega_{z_0}^{z}-\bar{M}_{z}^{z}K_{z}=(-\bar{M}_{z}^{z})_{max} \qquad (H)$$

Ultimately we can obtain the equations for the selection of K_z, K_i and K_n as follows:

$$K_z=-\left[\bar{X}_{f_{max}}-\bar{X}_f+\frac{m_z^{\bar{z}}}{\mu}\right]c_z^z/m_z^y \qquad (I)$$

$$K_z=KK_i$$

$$K_i=-\left(\frac{g}{l_z}-C\right)V/\left[g\,\bar{M}_z^y\left(1+\frac{V}{g}K\right)\right]$$

$$C=\frac{g}{V}\quad\frac{1}{\bar{Y}^y}(-\bar{M}_z^z)_{max}=-(m_z^y)_{max}\times\frac{mgb_A}{I_z}$$

Reference [4] recommends 0.02< K< 0.08. The results of the sample calculation indicate that the riding quality is better when K is close to the higher limit. In addition, according to the equation above the three feedback coefficients should be functions of the flight altitude and the M number. The calculation indicates, however, that they do not vary a lot within a flight range of M<1 so they can be set as constants.

II. SAMPLE CALCULATION

In order to verify that the feedback coefficients we have selected were reasonable, we have conducted a sample calculation by using a certain type of fighter plane as an example. We will now explain some of the results of the calculation.

1. Figure 2 indicates the variations of the feedback coefficients with the flight altitude and the M number. It can be seen from the figure that within the range of M<1.0, the K_{ao}, K_i and K_n varied only slightly with the altitude and the M number for the aircraft used in the sample calculation. We can set them to be constants in practical applications.

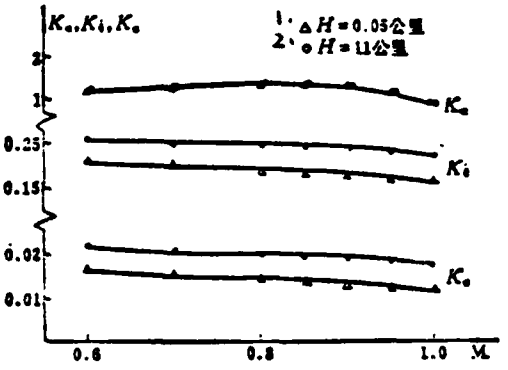

1. ΔH = 0.05 Km
2. $_{o}H$ = 11Km

Figure 2. Variation of the Feedback coefficients with the Mach number

2. After the three feedback coefficients are set to be constants, an example of the variation in the characteristics of the short period mode corresponding to the combined aircraft-SAS system is shown in Table 1. It can be seen from this table that a reasonable selection of the K_α, $K_{\dot\alpha}$, and K_n can increase the relative damping ratio and the intrinsic frequency at short periods, hence increasing the stability at short periods. At the same time, the sensitivity of the aircraft to the control reaction increases due to the increase in the intrinsic frequency and the CAP value. As for the effects of the feedback coefficients on the other control characteristics, they can be obtained by the reasonable selection of K_f and G. We will not discuss this aspect of the problem in the present paper.

3. The effect on the long period state by the introduction of the stability augmentation system. Table 2 lists the variations of the various coefficients in the characteristic equation before and after the combination of the sample aircraft

and the SAS. It can be seen that under the two kinds of flight conditions in Table 2, $a_4<0$ when the SAS is not installed and the long period mode is unstable. After the SAS is installed, $a_4>0$ and $R>0$ and the long period mode is stable.

4. The effect of the SAS on the riding quality of the aircraft. We have computed the following indices according to references [2,3]:

/21

H	3 情况 / 4 项目 M	5 无增稳器 ω_{du}(1/弧度)	ζ_{du}	CAP	7 有增稳器 ω(1/弧度)	ζ	CAP
2 (公里) 0.05	0.60	2.90	0.43	0.315	5.81	0.68	1.558
	0.70	3.17	0.46	0.281	6.84	0.65	1.583
	0.80	3.62	0.46	0.281	7.86	0.63	1.599
	0.85	3.87	0.46	0.282	8.38	0.61	1.610
	0.90	4.49	0.44	0.328	9.07	0.59	1.685
	0.99	5.53	0.37	0.436	10.01	0.55	1.841
	1.00	6.57	0.32	0.561	10.99	0.52	2.003

1. Table 1. The effect of the stability augmentation system on the characteristics of the short period mode

2. (kilometer)
3. condition
4. category
5. without the stability augmentation system
6. ω_{du} (1/radian)
7. with the stability augmentation system
8. ω (1/radian)

M	2-(H=0.05公里)	7-a_1(1/秒)	8-a_2(1/秒²)	9-a_3(1/秒³)	10-a_4(1/秒⁴)
0.9	3-无增稳器	4.0535	20.4629	1.2911	-0.1380
	4-加增稳器	7.8564	84.6440	5.8005	0.0408
0.95	5-无增稳器	4.2364	31.0515	3.3631	-0.0387
	6-加增稳器	8.3189	104.4355	11.5602	0.1143

1. Table 2. The effect of the stability augmentation system on the characteristics of the long period mode

2. (H=0.05 Km)
3. without the stability augmentation system
4. with the stability augmentation system added
5. without the stability augmentation system
6. with the stability augmentation system added
7. a_1 (1/second$_2$)
8. a_2 (1/second$_3$)
9. a_3 (1/second$_4$)
10. a_4 (1/second)

(1) Within each minute of the flight time, we will set the number of times in which the root means square value of the reaction of the normal directional acceleration of the pilot's position exceeds 0.5g to be N. The relationship between N and the evaluation of the passenger are as follows:

$N \leqslant 5$ comfortable

$5 < N \leqslant 13$ acceptable

$N > 13$ not acceptable

(2) The passenger work productivity index H_e. Reference [2] believes that He should be below 0.035. It believes that $\overline{H}_e$ 0.045 is unacceptable.

The computational results of the above mentioned indices for the sample aircraft are listed in Table 3.

H 3-增稳器 / M / 6-指标		0.6	0.7	0.8	0.85	0.9	0.95	1.0	7-备注
0.05 4-无	N	0	1	4	7	11	12	10	8 区<5
	$\bar{H}_e$	0.0754	0.0848	0.0956	0.1016	0.1129	0.1088	0.1010	9 区<0.045
2-(公里) 5-有	N	0	0	<3	<3	<3	<3	<3	10 区<5
	$\bar{H}_e$	0.0543	0.0470	0.0426	0.0425	0.0324	0.0440	0.0510	11 区<0.045

1. Table 3. The Riding Quality of the Sample Aircraft
2. (Km)
3. Stability augmentation system
4. without
5. with
6. index
7. remark
8. should be <5
9. should be <0.045
10. should be <5
11. should be <0.045

In this table, the following equation is used to compare the reaction of the normal-directional acceleration at the pilot's position /22

$$\Delta a_z = \bar{Y}^v_v \Delta v + \bar{Y}^v_\alpha \Delta\alpha + \frac{l_z}{g}\omega_z \qquad (J)$$

When the input quantities are selected as the V_g, α_g, and ω_x induced by the atmospheric turbulent flow, the frequency spectrum of Δa_n is

$$\Phi_e = G^*_{11}\Phi_{v_g v_g}G_{11} + G^*_{12}\Phi_{v_g \alpha_g}G_{12} + G^*_{13}\Phi_{v_g \omega_g}G_{13} + G^*_{13}\Phi_{\alpha_g v_g}G_{13} + G^*_{13}\Phi_{\alpha_g \alpha_g}G_{13} \qquad (K)$$

In this equation G_{11}, G_{12} , G_{13} used the V_g, α_g,ω_{xg} as input quantity, respectively. Δa_n is the transmission function corresponding to the output quantity. The footnote * indicates the complex conjugate.

The numerical computation indicates that Φ_n is primarily determined by the second term in the equation above.

It can be seen from Table 3 that the riding quality of the original aircraft was relatively poor under the computed flight state. The requirement of the riding quality index was bascially staisfied, however, after the stability augmentation system was introduced. This was due to the fact that the stability augmentation system increased the intrinsic frequencies at the center of energy distribution of the atmospheric turbulence. At the same time the stability augmentation system also increased the relative damping ratios at short periods. All these contributed to reduce the reaction of the normal-directional acceleration when the aircraft was flying within the atmospheric turbulence, hence improving the riding quality. From these points we can see that the method used by this paper to select the feedback coefficients of the longitudinal stability augmentation system can be applied in principle to the stability augmentation systems with the primary objectives of improving the riding qualities.

5. Reference [4] recommends that the working range (limit) of the stability augmentation system should be less than 10% of the maximum inclination angle of the flat tail. All the aircrafts used in the computation are within this range.

6. The variation in the dynamic characteristics of the combined aircraft-stability augmentation system within the contribution of the lift induced by the flat tail is considered.

As a result of the design of the exterior arrangement of the modern fighters, it is possible for the area of the flat tail to be close to 20% of the area of the wing. At this time we have to consider the variation in the lift induced by the

inclination of the flat tail, which is the $\bar{Y}^{b_z}\Delta\delta_z$ term. After taking this term into consideration, the short period transmission function of the aircraft is

(L)

$$\frac{\omega_z}{\Delta\delta_z} = \frac{L_\delta(T_1 S + 1)}{\Delta_{cm}}$$

$$\frac{\Delta\alpha}{\Delta\delta_z} = \frac{L_\alpha(T_\alpha S - 1)}{\Delta_{cm}}$$

$$\frac{\Delta n_y}{\Delta\delta_z} = \frac{L_\alpha(S^2 + 2\zeta_\alpha\omega_\alpha S + \omega_\alpha^2)}{\Delta_{cm}}$$

By comparing these results with the results which did not take the flat tail lift into consideration, we found that there is only a numerical quantity difference for $\omega_z/\Delta\delta_z$. For $\Delta\alpha/\Delta\delta_z$, there is an additional zero point in addition to a difference in quantity. There is an additional second order link on the numerator of $\Delta n_y/\Delta\delta_z$ and the characteristic equation remains unchanged. The computational results of the sample calculation indicate that when $\bar{Y}^{b_z} / \bar{Y}^{\alpha} \geq 0.20$ the above mentioned variation will induce relatively large variations in the dynamic characteristics of the combined aircraft-SAS system so it cannot be ignored.

III. CONCLUSIONS

1. For the longitudinal stability augmentation system with the main objective of improving the riding quality of the aircraft, we can select the feedback coefficients of the stability augmentation system by using the approximated condition that the reaction of normal-directional acceleration at the pilot's position be kept at a minimum. This type of combined aircraft-SAS system can satisfy the requirement of flight quality at both short and long periods, and it also assures that the aircraft has a good riding quality.

2. Within a range where the M number is not large, such as M <1, the feedback coefficients selected according to the procedures can be set as constants,and they also do not vary with the flight altitude.

3. If the area of the flat tail is large relative to the area of the wing, such as when $\overline{Y}^{b}_{z} / \overline{Y}^{\alpha} \geq 0.20$, we then have to consider the $\overline{Y}^{b}_{z}$ term for the analysis of the dynamic characteristics of the combined aircraft-SAS system.

REFERENCES /23

[1] Written by Atkin et al, translated by He Zhi Dai et al, Atmospheric Aerodynamics, Published by Scientific Publishing Company, Beijing (1979).

[2] J.W. Rustenburg, Development of Tracking Error Frequency Response Function and Aircraft Ride Quality Design Criteria for Vertical and Lateral Vibration, AD 719-514, Jan., (1971).

[3] Bruce G. Powers, Analytical Study of Ride Smoothing Benefits of Control System Configuration Optimized for Pilot Handling Qualities, NASA Tech. Paper, (1978), P 1148.

[4] G.S. Byushgens, R.V. Studnev. Aerodynamics of aircraft motion in longitudinal and roll motion. Mashinostroyenie, Moscow, 1979.

SELECTION OF SAS' LONGITUDINAL FEEDBACK COEFFICIENTS TO IMPROVE RIDING QUALITIES

Gao Hao

(Northwestern Polytechnical University)

Abstract

The longitudinal feedback coefficients of a stability augmentation system (SAS) for a sample aircraft were selected in the light of the condition that the normal acceleration response at the pilot's position approximated to zero. With the aid of references [2] and [3] the improvement in riding qualities of the airframe/SAS system due to the selected coefficients were evaluated. The dynamic characteristics of the airframe/SAS system were also analyzed.

The results demonstrate that the riding qualities are desirable when the control anticipative parameter of the airframe/SAS system approaches to $9.81/l_n$ and the operating range of the SAS is limited to the elevator displacement less than 10% of the max. displacement. It is necessary to take into account the lift due to the elevator deflection in the analysis of the dynamic characteristics of the airframe/SAS system, if the tail area is large enough in comparison with the wing area such as $\bar{Y}^{\delta_e}/\bar{Y}^{\alpha} \geqslant 0.2$.

The Compilation and Application of A State-Time Spectrum of Aircraft Ambient Vibration*

Nanchang Aircraft Manufacturing Company Gong Qing Xiang

ABSTRACT

The state-time spectrum of the aircraft vibration is an important statistical parameter of the aircraft. It is a prerequisite for inducing the ambient vibration data of an aircraft with the state inductive method. This paper proposes a compiling method for the state-time spectrum of aircraft ambient vibration. This method is based on the foundation of a great volume of flight statistical data, and it also fully considers both the flight condition in the air as well as the condition of the ground tests. The state-time spectrum of aircraft ambient vibration compiled this way can better represent the condition of the practical application of the aircraft. The compiling method has already been used in engineering applications.

SYMBOLS

A	the average ratio between the flight time and the time of ground tests per each flight
B	the number of ground tests within the life span of the aircraft
c	the number indicating the state of the ground test
m	the number indicating the flight course
l	number of aircrafts being included in the statistics
N_{ij}	the actual take off landing numbers of the i-th aircraft for the j-th course
N_j	the total actual take off landing numbers of all the aircrafts included in the statistics for the j-th course
N	the total actual take off landing numbers of all the aircrafts included in the statistics

*Received March, 1983

N_a the average take off landing numbers during the application life span of an aircraft

N_{sk} the take off landing numbers for a K-type typical course during the application life span of an aircraft

N_u the take off landing numbers of an aircraft within the application life span of the equipment loaded in the aircraft

p number of typical courses

r number of typical states

T_{ij} the flight time of the i-th aircraft for the j-th course

T_i the total flight time of all the aircrafts included in the statistics for the j-th course

T the total flight time of all the aircrafts included in the statistics

t the average time duration per flight

T_k the time used for the K-th type typical course by all the aircrafts included in the statistics

T_s the application life span of the aircraft on the onboard equipment

T_v the vibration life span of the onboard equipment

T_{sk} the flight time used for the K-th type typical course during the application life span of the aircraft

T_{kq} the time occupied by the Q-th type state during the flight for the K-th type typical course /25

T_q the time occupied by the Q-th type flight state during the application life span of the aircraft

t_Q the average time occupied by the Q-th type flight state per each flight

t_α the average time taken by the α-th ground test state per each flight

T_α the time taken by the α-th grcund test state during the application life span of the aircraft

t_e the average time necessary to conducted an extended vibration experiment per each flight

T_e the time used for the extended vibration experiments for the onboard equipment with an application life span of T_s

t_g the average time used for each ground test

t_k the time used for the k-th type typical course per flight

V_x the average time taken by the x-th ground test state per each ground test process

W_q the value of random vibration corresponding to the Q-th type typical state

W_{max} the maximum value of random vibration of all the typical states

I. INTRODUCTION

In order to specify the experimental standards of the onboard equipment and the vibration of the instruments it is necessary to conduct vibration experiments on the aircraft Then we can proceed to analyze the original vibration data measured during the experiments. In addition, it is necessary for us to use the appropriate statistical methods to synthesize and induce the large amount of analytical data. Only by doing this can we come up with the basic experimental parameters necessary for specifying the vibration standards.

Before the 1970's, most of the induction of the ambient vibration data applied the "peak value inclusion method". On a piece of graph paper with value of vibration versus frequency, the "peak value inclusion method" picks a curve which contains

most of the data points while rejecting a minority of isolated data points which stuck out as the standard vibration curve[1]. This method is very easy to do but its drawback is that its inductive result is too crude and conservative. At the same time it is also difficult to reasonably specify the time of the vibration experiment[1].

Based on a series of research into the various data inductive methods available to date, the present paper proposes the inductive method for the experimental data collected from the aircraft ambient vibration experiment - the state inductive method. The results obtained by using this inductive method can better reflect the synthesized vibration characteristics, and it is relatively non-conservative. In addition, this method introduces the view point of the limited life span design. In other words, the time of the function experiment and the time of the extended experiment are determined according to the actual time duration of the various states. This makes the specification of the time of vibration experiment more reasonable and reliable. This is why the state inductive method is more advanced and reasonable when compared with the peak value inclusion method.

It is necessary for us to know the state-time spectrum of the aircraft ambient vibration in order to apply the state inductive method. This is to say that we have to know the times taken up by the various typical states of the aircraft during each average flight.

The state-time spectrum of the aircraft ambient vibration is an important statistical parameter. Similar to the loading fatigue spectrum of the aircraft, it is obtained statistically by using the actual flight data of the aircraft. There are, however, major differences between the two: 1. the loading fatigue spectrum gives the repeated number of every degrees of overloading values during the application life span of the aircraft, while the state-time spectrum gives the times

occupied by every type of typical states (such as taxiing during take-off, climbing, cruising, diving, and spiraling) during each average flight. 2. The compilation of the loading fatigue spectrum does not take the conditions of the ground tests into consideration. However, the vibration caused by the ground tests can induce the same kinds of damage and destruction to the products. The actual measured data indicates that for certain parts of the aircraft the value of vibration caused by the ground tests was even greater than that produced during the flight. This is why the construction of the state-time spectrum of aircraft ambient vibration will have to simultaneously consider both the conditions in the air as well as the ground test conditions.

The aircraft is an aviation vehicle that will be used repeatedly. There are many different kinds of flight courses and the flight states are also complicated. This paper presents a method for the compilation of the state-time spectrum of aircraft ambient vibration. This method is established on the foundation of large amounts of flight statistical data, and it also fully considers both the flight condition in the air as well as the ground test condition. The state-time spectrum of aircraft ambient vibration compiled this way can better reflect the actual /26 application condition of the aircraft. We will now introduce the compiling method as follows.

II. COMPILING PROCEDURES

1. After checking the flight records of the aircrafts involved in the statistics, the following data are computed statistically:

(1) the actual numbers of take offs and landings of each aircraft for each course N_{ij} and the corresponding flight time T_{ij}.

(2) the numbers of take offs and landings of all the aircrafts involved in the statistics for each course N_j and the flight time T_j

$$N_j = \sum_{i=1}^{l} N_{ij} \tag{1}$$

$$T_j = \sum_{i=1}^{l} T_{ij} \tag{2}$$

(3) the actual numbers of total take offs and landings of all the aircrafts involved in the statistics N and the total flight time T:

$$N = \sum_{j=1}^{m} N_j \tag{3}$$

$$T = \sum_{j=1}^{m} T_j \tag{4}$$

2. After checking the record of the propeller of the aircraft (if an aircraft has two or more propellers, only the record of one of the propellers will be included in the statistics), the ratio between the flight time for an average flight (including take off, landing and taxiing) and the time for the ground test is statistically computed to be A:1.

In order to assure statistical accuracy, the numbers of aircrafts and propellers generally should not be less than 30.

3. The time required to complete an average flight is computed as

$$t = \frac{T}{N}\left(1 + \frac{1}{A}\right) \tag{5}$$

4. The combined classification of the flight courses: there are many different kinds of flight courses during the actual training. However, some of the contents of these courses are the same or similar to one another from the view point of ambient vibration,so they can be combined. The principles used

to combine these courses are: the corresponding flight time, flight altitude, flight velocity and the flight motion should be roughly similar for courses which are combined into the same category. After the combined classification, the course with the highest numbers of actual flights in each category will be used to represent a typical flight course in the same category.

By adding the flight times of the courses in the same category, we can compute statistically the flight time of the K-th category courses for all the aircrafts involved in the statistics T_k.

Assume that the application life span of the aircraft is T_s, the flight time for each category within T_s is

$$T_{sk}=\frac{T_k}{T}T_s \quad (K=1,2,\cdots,p) \tag{6}$$

We can convert T_{sk} into the take off and landing numbers for the typical flight course of that particular category as

$$N_{sk}=T_{sk}/t_k \quad (K=1,2,\cdots,p) \tag{7}$$

5. Two methods can be used to plot out the state-time cross-section of a typical flight course: one way is to conduct test flight experiment for each typical course, measure the time records of the flight parameters such as the flight altitude, velocity, flight posture, pressure and longitudinal loading throughout the entire flight process from take off taxiing to landing taxiing; the other method is to conduct theoretical estimation. It does not matter whether we apply one method over the other, or if we use both methods, the objective is to measure /27 or estimate the time occupied by each flight state in each typical course as well as the corresponding flight altitude, velocity, pressure, and the longitudinal loading value. In this way, we can obtain the state-time cross-section of each typical course.

6. The combination of the flight states: the aircraft will have to perform a lot of flight motions during the actual flight process. At the same time, due to the differences in the state of the aircraft's propeller and flight parameters such as flight altitude, velocity, and longitudinal loading value, the flight state of the aircraft will change at all times. It is necessary for us to combine and classify them in order to proceed with the statistical analysis. The principles for the classification are: (1) the flight motions of the flight states in the same category will have to be the same or similar; (2) the flight altitude will be divided into low, medium and high altitude ranges, the flight altitudes of the flight states in the same category will have to be within the same altitude range; (3) the flight velocity will be divided into 3 to 5 levels according to the magnitude of the velocity, the flight velocities of the flight states in the same category will have to be within the range of the same level.

7. By adding the flight times of the various states which belong to the same state category and the same course category, we can obtain the time occupied by each category of flight state for each category of course T_{kQ} (K = 1,2,...,p, Q = 1,2,...r).

8. We can compute the time occupied by each flight state category within T_s as

$$T_0 = \sum_{k=1}^{p} T_{KQ} N_{sk} \qquad (8)$$

9. According to the propeller's ground test curve we can obtain the time occupied by each test state (such as slow rate, specified rate, maximum and acceleration) per each ground test process V_a (a = 1,2,..., c).

2. 序号	3. 空域	6. 典型状态名称	7. 平均一次飞行中所占的时间（分）	28 序号	29 空域	33 典型状态名称	34 平均一次飞行中所占的时间（分）
1		7. 起飞滑跑	0.430	21	30 中空空域	34 平飞速度 3	2.605
2		8. 着陆滑跑	0.463	22		35 平飞速度 4	0.589
3	4. 低空空域	9. 爬升	2.688	23	31 高空空域	36 爬升	0.106
4		10. 盘旋	3.437	24		37 盘旋	0.429
5		11. 俯冲跃升	1.068	25		38 俯冲跃升	0.144
6		12. 上升转弯	2.122	26		39 上升转弯	0.136
7		13. 下滑	0.553	27		40 下滑	0.126
8		14. 平飞速度 1	1.161	28		41 截击	0.010
9		15. 平飞速度 2	6.750	29		42 平飞速度 1	0.061
10		16. 平飞速度 3	0.291	30		43 平飞速度 2	0.001
11		17. 空战格斗	1.190	31	32 地面试车	44 怠车	0.833
12		18. 攻强度	1.892	32		45 放气活门打开	0.417
13	5. 中空空域	19. 爬升	1.345	33		46 放气活门关闭	2.636
14		20. 盘旋	1.792	34		47 右发慢车	0.833
15		21. 俯冲跃升	0.841	35		48 右发加大	0.138
16		22. 上升转弯	0.368	36		49 右发额力	0.138
17		23. 下滑	1.053	37		50 左发慢车	0.833
18		24. 截击	0.039	38		51 左发加大	0.138
19		25. 平飞速度 1	0.002	39		52 左发额力	0.138
20		26. 平飞速度 2	2.238	40		53 加减油门	0.555

1. Table 1. An example of the state-time spectrum of the ambient vibration of the aircraft

2. serial number
3. air space
4. low altitude air space
5. medium altitude air space
6. names of the typical states
7. take off taxiing
8. landing taxiing
9. climbing
10. spiraling
11. diving and rapid climbing
12. turning and increase altitude
13. gliding downward

14. cruising velocity 1
15. cruising velocity 2
16. cruising velocity 3
17. put down the landing gear
18. put down the wing flaps
19. climbing
20. spiraling
21. diving and rapid climbing
22. turning and increase altitude
23. gliding downward
24. horizontal rolling
25. cruising velocity 1
26. cruising velocity 2
27. the time used for each average flight (minutes)
28. serial number
29. air space
30. medium altitude air space
31. high altitude air space
32. ground tests
33. names of the typical states
34. cruising velocity 3
35. cruising velocity 4
36. climbing
37. spiraling
38. diving and rapid climbing
39. turning and increase altitude
40. gliding downward
41. horizontal rolling
42. cruising velocity 1
43. cruising velocity 2
44. slow rate
45. open the gas release belt
46. close the gas release belt
47. right propeller at constant rate
48. right propeller at maximum rate
49. right propeller thrust
50. left propeller at constant rate
51. left propeller at maximum rate
52. left propeller thrust
53. property of acceleration or deceleration
54. the time used per each average flight (minute)

We already know that the time required for each ground test /28 is t_g, the necessary numbers of ground tests within T_s is thus

$$B = \left(\frac{T_s}{A}\right)/t_g \qquad (9)$$

The times in which the aircraft is in the various test states within T_s are

$$T_\alpha = V_\alpha B \quad (\alpha = 1, 2, \cdots, c) \tag{10}$$

10. We can compute the average numbers of take off and landing within T_s as

$$N_\alpha = T_s\left(1 + \frac{1}{A}\right)/t \tag{11}$$

11. The time occupied by each state for each average flight process is thus

$$t_Q = T_Q/N_\alpha \ (Q = 1, 2, \cdots, p) \tag{12}$$

$$t_\alpha = T_\alpha/N_\alpha \ (\alpha = 1, 2, \cdots, c) \tag{13}$$

This is the required state-time spectrum of the ambient vibration of the aircraft.

Table 1 shows one example of the state-time spectrum of the ambient vibration of the aircraft.

III. EXAMPLES OF APPLICATION

1. If we already know the application life span T_s of the aircraft or the on board equipment, the state-time spectrum of the ambient vibration of the aircraft, as well as the random vibration quantity W_Q (Q = 1,2,...,r) (g^2/H_z) experimentally for this particular equipment for each state, we can determine the measured value and time of the vibration experiment corresponding to that particular equipment.

Reference [1] specifies that the maximum W_{max} among all the W_o be selected as the measured value for the function experiment. It also specifies that we should select a state corresponding to W_{max} from the state-time spectrum and set the time of an actual flight at that particular state.

If we set the measured value for the extended experiment to be W_{max} as well, the time required for the extended experiment per each average flight is

$$t_e = \sum_{Q=1}^{r} \left(\frac{W_Q}{W_{max}}\right)^k T_Q \qquad (14)$$

The take off and landing numbers of the aircraft within T_s are

$$N_e = T_s\left(1 + \frac{1}{A}\right)/t \qquad (15)$$

The time of the extended duration experiment necessary for that particular equipment is thus

$$T_e = t_e N_e \qquad (16)$$

2. To determine the vibrational life span of the on board equipment, a certain piece of equipment will suffer unacceptable damage or destruction after it has been subjected to a vibration quantity W_{max} for a time of T_e. Now we will determine the vibrational life span of that particular piece of equipment.

Based on the state-time spectrum of the ambient vibration of the aircraft, we can obtain the time te necessary to conduct an extended duration experiment for that particular piece of equipment per each average flight from equation (14).

In this way, the vibrational life span of that piece of on board equipment can be determined by the equation below:

$$T_r = \frac{T_e}{t_e} t \qquad (17)$$

As we all know, the application life span of the on board equipment is determined by many factors. In addition to the fatigue damage induced by vibration, factors such as wearing, corrosion and mould can all cause the equipment to lose the functional capability. If the vibrational life span T_r computed from equation (17) is smaller than the application life span /29

computed based on other factors, we should use the vibrational life span T_v to determine the replacement period of that particular piece of on board equipment.

REFERENCES

[1] Yao Qi Hang: A synthesized description of the problems related to the specification of standards for the ambient vibration experiments, Standardized aero-aviation, 2, (1980).

COMPILATION AND APPLICATION OF A STATE-TIME SPECTRUM OF AIRCRAFT AMBIENT VIBRATION

Gong Qingxiang

(*Nanchang Aircraft Manufactoring Company*)

Abstract

A state-time spectrum of aircraft ambient vibration is an important statistical parameter of an aircraft. It is an essential precondition for inducing ambient vibration data of an aircraft with the state inductive method.

This paper puts forward a compiling method of the state-time spectrum of aircraft ambient vibration. It is based on a great deal of statistical data taking both flight and ground tests into comprehensive consideration. Therefore, the state-time spectrum of aircraft ambient vibration drawn up by this method can give true expression of the aircraft practice.

This method has found engineering application.

END

FILMED

1-85

DTIC